Acta Biochim Biophys Sin 2014, 46: 273–282 | © The Author 2014. Published by ABBS Editorial Office in association with Oxford University Press on behalf of the Institute of Biochemistry and Cell Biology, Shanghai Institutes for Biological Sciences, Chinese Academy of Sciences. DOI: 10.1093/abbs/gmt155.
Advance Access Publication 27 January 2014

Original Article

Role of plasma membrane lipid composition on cellular homeostasis: learning from cell line models expressing fatty acid desaturases

María S. Jaureguiberry[1,2], M. Alejandra Tricerri[1,2]*, Susana A. Sanchez[3], Gabriela S. Finarelli[1,2], Mauro A. Montanaro[1,2], Eduardo D. Prieto[1], and Omar J. Rimoldi[1,2]

[1]Instituto de Investigaciones Bioquímicas de La Plata (INIBIOLP), La Plata 1900, Buenos Aires, Argentina
[2]Facultad de Ciencias Médicas, Universidad Nacional de La Plata, Calles 60 y 120, La Plata 1900, Buenos Aires, Argentina
[3]Laboratory for Fluorescence Dynamics (LFD), University of California, Irvine, CA 92697-2715, USA
*Correspondence address. Tel: +54-221-4824894; Fax: +54-221-4258988; E-mail: aletricerri@yahoo.com

Experimental evidence has suggested that plasma membrane (PM)-associated signaling and hence cell metabolism and viability depend on lipid composition and organization. The aim of the present work is to develop a cell model to study the endogenous polyunsaturated fatty acids (PUFAs) effect on PM properties and analyze its influence on cholesterol (Chol) homeostasis. We have previously shown that by using a cell line over-expressing stearoyl-CoA-desaturase, membrane composition and organization coordinate cellular pathways involved in Chol efflux and cell viability by different mechanisms. Now, we expanded our studies to a cell model over-expressing both Δ5 and Δ6 desaturases, which resulted in a permanently higher PUFA content in PM. Furthermore, this cell line showed increased PM fluidity, Chol storage, and mitochondrial activity. In addition, human apolipoprotein A-I-mediated Chol removal was less efficient in these cells than in the corresponding control. Taken together, our results suggested that the cell functionality is preserved by regulating PM organization and Chol exportation and homeostasis.

Keywords membrane heterogeneity; fatty acid desaturases; cholesterol transport; cytotoxicity; human apolipoprotein A-I

Received: September 4, 2013 Accepted: November 19, 2013

Introduction

Disorders in lipid metabolism underlie many current pathologies in western lifestyle, such as metabolic syndrome and cardiovascular disease. The cause seems to be in part related to western diet, typically enriched in refined sugars, cholesterol (Chol), and saturated fatty acids (FAs). In addition, the role of polyunsaturated fatty acid (PUFA) in this kind of diet has been extensively analyzed, but its particular effect is still far from being clear. For instance, while different reports agreed on the benefit of consuming lower levels of n-6 PUFA, there is no unanimity whether higher or lower ingestion of n-3 PUFA would decrease the incidence of the mentioned pathologies [1–4]. While some PUFAs are known for their anti-inflammatory and anti-oxidant action, Cavaliere and docosahexaenoic acid (DHA) has been even proposed as 'a promising tool for preventing age-related brain deterioration' [5]; a recent study has showed that in cerebrovascular inflammation, a diet enriched in DHA worsens blood–brain barrier integrity already compromised by chronic ingestion of saturated fats [6]. Endogenous n-3 and n-6 PUFA are derived from diet essential FAs, α-linolenic (18 : 3, n-3) and linoleic (18 : 2, n-6), respectively, by the activity of FA desaturases Δ5 (FADS1) and Δ6 (FADS2) in a coordinated mechanism with elongases. Furthermore, it has been proposed that the *FADS2* gene product would also have Δ8-desaturase activity converting 20 : 2 (n-6) to 20 : 3 (n-6) and 20 : 3 (n-3) to 20 : 4 (n-3). The activity of these enzymes results in the synthesis of physiologically relevant FAs such as arachidonic acid (20 : 4, n-6), eicosapentaenoic acid (20 : 5, n-3), and DHA (22 : 6, n-3). The pathways by which PUFAs exert their action are certainly diverse; they regulate gene expression as ligands of important transcription factors such as liver X receptor, sterol response element binding protein-2 (SREBP-2), and peroxisome proliferator activated receptor [7], and they also render pro- (n-6 PUFA) and anti- (n-3 PUFA) inflammatory mediators through eicosanoid metabolism [4,8,9].

Evidence that PUFAs alter membrane composition and modulate microdomain organization and signaling has been published some years ago [10], and it is still a topic of important debate [3,11,12]. In the past few years, evidence has been accumulated supporting the model for plasma membrane (PM) organization with transient and rapidly changing microdomains that allow the interaction of resident proteins and lipids nearby [13–15].

Assembly of lipid domains is the consequence of different affinities among lipids or between lipids and membrane

proteins. The best documented example in biological membranes is the coexistence of segregated fluid–fluid domains composed of Chol and sphingomyelin (SM)-rich or Chol-poor phases. In addition to this heterogeneity and because of the large number of chemical species coexisting in a membrane, small amounts of certain lipids could introduce extra domain segregation thus affecting membrane structure, dynamic, and function. For example, very long-chain PUFA, sometimes even referred to as 'cholesterol-phobic', form membrane domains containing very little sterol due to sterical incompatibility [11]. The selective partition of proteins into specific membrane domains and consequently the regulation of some signaling pathways associated to these events are likely to depend on changes in the membrane composition and organization.

Since there has been experimental evidence showing that membrane structure is dramatically altered by changes in PUFA content [11], our aim was to obtain and characterize a cell model with elevated levels of endogenous PUFA to study Chol homeostasis and membrane properties. Therefore, we constructed a stable cell line over-expressing rat FADS1 along with FADS2, which resulted in a relative increase of PUFA with respect to the monounsaturated fatty acid (MUFA) at the PM. The permanent modification in the PM lipids achieved in this model overcame inconveniences of most studies which analyzed the effect of exogenous PUFA added to the medium in cell culture experiments or through specific diet formulation in animal models. We characterized PM properties, Chol removal and storage, and discussed our results in terms of lipid rearrangement and cell cytotoxicity.

Materials and Methods

Materials

Human apolipoprotein A-I (apoA-I) from the plasma of healthy donors (kindly donated by Banco de Sangre, Instituto de Hemoterapia de la Provincia de Buenos Aires, La Plata, Argentina) was isolated and purified as previously described [16]. Purity was higher than 95% as estimated by sodium dodecyl sulfate–polyacrylamide gel electrophoresis using Coomassie blue staining. Laurdan [6-lauroyl-2-(dimethylamino) naphthalene], was purchased from Molecular Probes (Eugene, USA). Bovine serum albumin (BSA), Tris(hydroxymethyl)aminomethane hydrochloride (Trizma® HCl), 3-(4,5-dimethylthiazol-2-yl)-2,5-diphenyl tetrazolium bromide (MTT), and lipids used as standards for thin layer chromatography (TLC) (egg phosphatidylcholine, free and esterified Chol, brain SM, phosphatidylinositol, phosphatidylserine, and phosphatidylethanolamine) were obtained from Sigma-Aldrich Biochemicals (St Louis, USA); minimal essential medium (MEM) and the antibiotic-antimycotic mixture were obtained from Invitrogen Corporation (Carlsbad, USA). Fetal bovine serum (FBS) was purchased from Bioser (Buenos Aires, Argentina) and 1,2-^{3}H(N)-cholesterol was obtained from Amersham Biosciences (Pittsburgh, USA). Chinese hamster ovary (CHO) cells (CHO-KI) were purchased from ATCC (CCL-61; Manassas, USA).

Construction of a stable cell line over-expressing Δ5 and Δ6 desaturases

Rat Δ5 (FADS1) desaturase cDNA [17] was subcloned into the mammalian expression vector pcDNA3.1/geneticin (Invitrogen) and transfected into CHO-KI cells by using Lipofect-AMINE 2000 (Invitrogen). Transfectants expressing Δ5 desaturase were selected with geneticin (200 μg/ml). The clone with the highest Δ5 desaturase expression level (assessed by Northern blot, data not shown) was further transfected with the vector construct pcDNA 3.1/Hygro (Invitrogen) containing the full-length rat Δ6 desaturase (FADS2) [18]. A clone resistant to both geneticin and hygromycin (200 μg/ml) was selected, expanded, and frozen in liquid N_2 for further experiments. The resistant clone was designated as FADS cells. In addition, cells transfected with the plasmids without the desaturases inserts were considered as control for all experiments.

Quantitative real-time polymerase chain reaction

Desaturase gene expression level was determined by real-time polymerase chain reaction (RT-PCR). Total RNA was isolated from control and FADS cells ($n = 5$ in each group) by using Trizol reagent (Invitrogen). Isolated RNA (1.5 μg) was separated on 1.0% agarose-1 M formaldehyde gel electrophoresis to assess RNA quality. Quantitative RT-PCR analysis was performed by using an MX3000 apparatus (Stratagene, La Jolla, USA). Total RNA (1 μg) from individual samples was used to generate cDNA by using the Affinity Script QPCR cDNA kit (Stratagene). Equal amounts of cDNA were amplified with Brilliant SYBR Green QPCR Master Mix (Stratagene). The levels of various mRNAs were normalized to those of β-actin. The quantitative RT-PCR primers were as follows: Δ6 desaturase 5′-TGTCCACAAGTTTGTCATTGG-3′ (forward) and 5′-ACACGTGCAGGTCTTTATG-3′ (reverse); Δ5 desaturase 5′-TGGAGAGCAACTGGTTTGTG-3′ (forward) and 5′-GTTGAAGGCTGACTGGTGAA-3′ (reverse); β-actin, 5′-TGTCAGCAATGCCTGGGTACA-3′ (forward) and 5′-ACTATTGGCAACGAGCGGTT-3′ (reverse).

Cell culture

Cells were cultured as previously described [19]. Briefly, CHO cells were seeded into 10 cm diameter culture dishes and incubated until confluence in MEM supplemented with penicillin/streptomycin solution (100 units/ml) and 10% FBS at 37°C in a 5% CO_2 atmosphere.

Membrane isolation and lipid composition analysis

To isolate PM, we followed the technique of Mander *et al*. [20] with further modifications as previously described [19]. Lipids were quantified by TLC and FAs were analyzed by gas liquid chromatography [19].

[^{3}H] Chol labeling of cells and Chol efflux assays

Cells were labeled and loaded or not with Chol at the same time by overnight incubation with 0.5 μCi/ml [^{3}H] Chol in serum-free medium supplemented with or without 50 μg/ml Chol as described above. After 24 h equilibration with 2 mg/ml BSA-MEM, monolayers were washed with PBS and treated for 12 h with serum-free medium containing 12 μg/ml of apoA-I or not. Aliquots of the medium were collected stepwise at different time periods and a final aliquot was collected after 24 h incubation for scintillation counting. Finally, cells were scrapped and resuspended in PBS for scintillation counting as well. In a different assay, cells were scrapped after labeling and incubation as described, lipids were extracted, and sterol species were separated by high-performance TLC on a silica gel plate with concentrating zone (Whatman, Schleier-Schuell, UK). Membrane lipid mixtures were developed in hexane/ethyl ether/acetic acid (80 : 20 : 1, v:v), and spots corresponding to cholesteryl esters (CE) and unesterified Chol (FC) were identified by staining with I_2 vapor and co-migration with authentic standards. Appropriate spots were scraped and quantified by scintillation counting.

Cell functionality

Control and FADS cells were incubated as described above in multiwell plates. Then, the MTT assay was carried out as previously described by Mosmann [21] with modifications. Briefly, cells were grown under different experimental conditions and then incubated with 0.5 mg/ml MTT in PBS at 37°C for 4 h to allow MTT reduction to formazan blue by metabolically active cells. Next, crystals were solubilized and formazan was quantified as optical density (OD) increase at 570 nm in a DTX 880 multimode detector (Beckman Coulter, Fullerton, USA).

Laurdan generalized polarization imaging and quantification

A full discussion of the use and mathematical significance of generalized polarization (GP) can be found in the literatures [22–25]. Briefly, Laurdan is used as a membrane probe because of its large excited-state dipole moment, which enables it to report the extent of water penetration into the bilayer surface as a result of dipolar relaxation [26]. Water penetration has been correlated with lipid packing and membrane fluidity [27]. If Laurdan is solubilized in a lipid structure (i.e. a membrane), its spectrum senses the environment and shifts according to the water content of the bilayer. The quantification of the spectral shift is given by (1):

$$\mathrm{GP} = (I_{440} - I_{490})/(I_{440} + I_{490}) \quad (1)$$

where I_{440} and I_{490} are the emission intensities at 440 and 490 nm, respectively. Images were collected on a scanning two-photon fluorescence microscope designed at the Laboratory for Fluorescence Dynamics (University of California at Irvine, USA) as previously described [25,28]. The fluorescence was split into two channels by using a Chroma Technology 470 DCXR-BS dichroic beam splitter in the emission path. Interference filters (Ealing 490 and Ealing 440) were placed in the emission paths to further isolate the two desired regions of the emission spectrum. Two simultaneous emission images (centered at 440 and 490 nm) were obtained from the cells, which were processed applying the GP formula (1) to each pixel using the SimFCS program (Laboratory for Fluorescence Dynamics). Corrections for the wavelength dependence of the emission detection system were accomplished through the comparison of the GP value of a known solution (Laurdan in dimethyl sulfoxide) [29]. FADS or control cells were grown as previously described until 70% confluence (in order to allow observation of single cell membranes) and then loaded or not with Chol as mentioned above. Subsequently, cells were washed with PBS and incubated for 15 min at 37°C with Laurdan to a final concentration of 1 μM in Dulbecco's modified Eagle's medium (DMEM) + 2.5% FBS. After rinsing three times with fresh medium, cells were kept in DMEM at the same temperature during the observation time in a thermostatized microscope stage. To avoid data dispersion due to laser alignment, cell confluence, and so on, treatments were compared with untreated cells measured over the same day and under same conditions [19].

Statistical analysis

Unless otherwise stated, results were shown as the mean ± SE of at least three independent measurements. Normality could not be proved in any case, and therefore statistically significant differences among sample means were evaluated by the Mann–Whitney *U* test (*$P < 0.05$ vs. control). Variances were similar for all pair of groups tested ($P > 0.05$, *F* test).

Results

Cell line construction and characterization

To obtain a reliable cellular model to test the influence of membrane composition on Chol homeostasis and cell functionality, a cell line was constructed showing stable PUFA-enriched lipid composition at the PM. The efficiencies of FADS1 and FADS2 transfection and over-expression were confirmed by quantitative RT-PCR, showing that mRNA levels of both desaturases increased more than five

times in the transfected cells, when compared with control (**Fig. 1A,B**). Then, to verify that the over-expression resulted in a higher activity of both enzymes, we analyzed membrane FAs composition. As expected, the combined activity of both desaturases induced a significant increase (41%) in the poly vs. monounsaturated fatty acids (PUFA/MUFA) ratio, when compared with the control (**Fig. 1C**). In addition, we analyzed the relative composition of the major lipid classes at the membrane. To simplify comparative studies, data were expressed as the mass ratio of glycerophospholipids (PL) to SM, and glycerophospholipids to FC [19]. As shown in **Fig. 1D**, PL/SM and PL/FC ratios were higher by 74% and 60%, respectively, in FADS cells, when compared with control, indicating a lower relative content of FC and SM in response to PUFA build up.

Membrane organization of cells *in vivo*

Given the different lipid composition of FADS cells as compared with the control, we analyzed the PM organization of both cell types in living cells. We have previously addressed this issue in a different cell type using Laurdan GP imaging and two-photon excitation fluorescence microscopy [19,24,30,31]. Laurdan partitions equally into fluid or condensed membranes and is not associated to specific FAs or phospholipid head groups [22]. Hence, GP values reflect the overall membrane organization and not a specific lipid or protein composition [32], simplifying the analysis of lateral organization. According to the method previously described [19], Laurdan-labeled cells were observed by setting the focal *z* plane in the middle of the cell, a configuration that allows the observation and GP measurements at the PM. GP values

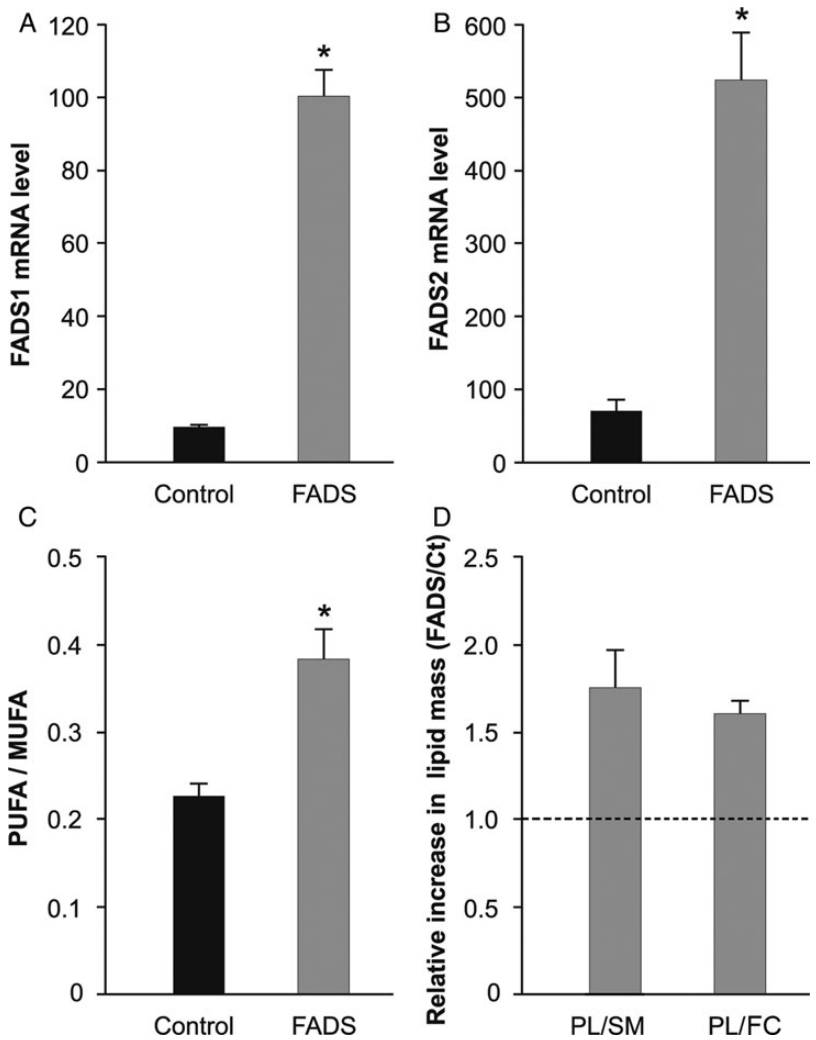

Figure 1. Fatty acid desaturases effect on membrane composition (A,B) Quantification of mRNA levels by quantitative RT-PCR. Gray bars represent mRNA levels in FADS1 cells (A) and FADS2 cells (B) and black bars in control cells. (C) Comparative FA composition of FADS (gray) vs. control (black) cells. PUFA/MUFA ratio increased 41% in FADS cells. (D) Relative composition of major lipid classes at the PM. PM lipids were separated by TLC and the composition was quantified by scanning of different lipid areas after calcination. Figure showed relative ratios of glycerophospholipids (PL) to SM and to FC in FADS cells with respect to control. Dashed line showed ratio = 1, to better visualize the relative changes induced by the over-expression of FADS1 and FADS2. In FADS cells, PM both PL/SM and PL/FC ratios were higher by 74% and 60%, respectively, when compared with the control cells, indicating a relative lower FC and SM content in the PM of the transfected cells. $*P < 0.05$ vs. control cells.

ranged from 1 to −1 according to (1). The analysis of a GP image was shown in **Fig. 2A**. In a typical GP image of a CHO cell (**Fig. 2A**, 1), two areas can be easily distinguished: pixels with high GP values (orange) and low GP values (yellow) corresponding to the PM and internal membranes, respectively [31]. The pixel distribution (GP histogram) from this image (**Fig. 2A**, 2) also showed two populations: one pick centered on GP values around zero (internal membranes) and a second one centered on GP values around 0.3 (PM). By using the Image J software, we isolated the pixels corresponding to the PM from the image (**Fig. 2A**, 3) and used the corresponding histogram (**Fig. 2A**, 4) to analyze the PM organization. The center of the PM pixel distribution (**Fig. 2A**, 4) was the average GP value and could be interpreted as the average fluidity of the PM. FADS cells showed a statistically significant decrease of average GP values, when compared with control cells, implying higher fluidity (higher water content in the PM) (**Fig. 2B**). To further understand the origin of this difference in PM fluidity, we applied the coverage analysis [33]. In this analysis, the pixel distribution corresponding to PM was deconvoluted into two best-fitted Gaussians (**Fig. 2C**), and the obtained parameters (Areas 1 and 2) and mean GP values (1 and 2) were plotted as percentage coverage vs. main GP value, respectively. It is important to mention that in this type of analysis, the thickness of the PM has to be assigned. PM is around 6–7 nm, the point spread function of the two-photon system is around 300 nm, therefore, the areas adjacent to the PM will contribute to the signal. We assigned the area corresponding to the PM based on the GP value, as well as previous studies using giant unilamellar vesicles [24,34] and red blood cells [31,35], systems where the contribution of the cytosol is zero or minimal.

This coverage plot was interpreted as a map of the distribution of two populations of lipid domains having different mean GP values: low (L-GP, more fluid) and high (H-GP, less fluid) mean GP. GP-domain population composition

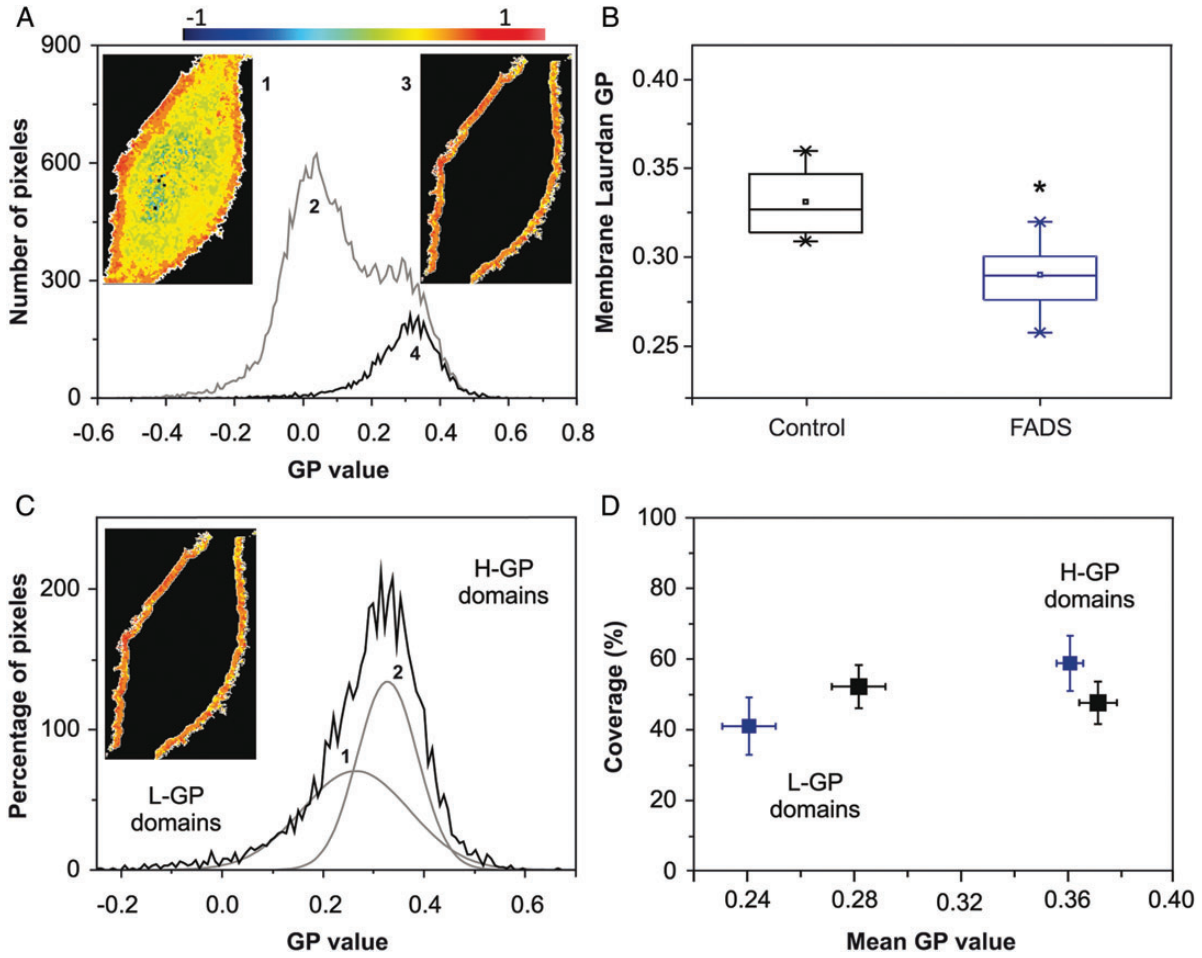

Figure 2. PM organization (Laurdan GP imaging) (A) Average Laurdan GP value for the PM is obtained from the GP image (1) taken at the middle plane of the cell. In the pixel distribution (2) the pixels corresponding to the membrane (3) were isolated for analysis (4). (B) Average membrane GP values from control and FADS cells. Box charts showed minimum, median, 25th, and 75th percentile values. *$P<0.05$. (C) Pixels distribution from the PM (image inserted) is deconvoluted into two best-fitted Gaussians and the area and main GP value of each Gaussian distribution are obtained. (D) Double plot where the center of each Gaussian (main GP value) and the area (% coverage) was represented for 15 cells. All measurements were performed at 37°C. Black and blue plots represented control and FADS cells, respectively.

obtained by this procedure (**Fig. 2D**) showed clear difference between control and FADS cells. In control cells (black symbols), there was similar percentage coverage for the two populations with average GP values of 0.28 ± 0.05 (L-GP) and 0.37 ± 0.03 (H-GP). Instead, for FADS cells (blue symbols), the main GP value of the H-GP domains remained similar to that of control cells with ~60% of the number of pixels, but the L-GP domains showed a significant decrease in main GP value (from 0.28 to 0.24 ± 0.05) and a 10% coverage reduction. These results indicated that the higher fluidity observed in PM from FADS cells was mainly due to an increased fluidity of more fluid domains (L-GP).

Chol efflux

We next examined the effect of increased desaturases expression on cellular Chol efflux mediated by lipid-free apoA-I. The first step of lipid removal by apoA-I is an active process mediated by the ATP-binding cassette transporter A1 (ABCA1), which preferentially partitions into liquid-disordered domains [36]. It is well known that apoA-I is efficient to remove Chol from cells in a time-dependent fashion [37]. Results showed that after 24 h incubation, apoA-I removed about 30% of the loaded Chol from control cells, and about 20% from FADS cells under the same conditions (**Fig. 3A**). A similar trend was observed on comparing Chol-loaded cells (data not shown).

Intracellular Chol esterification

The decreased efficiency of Chol removal by apoA-I from FADS cells might be due to the reduced amount of Chol in the PM with respect to the control (**Fig. 1**). However, it was also possible that the equilibrium between FC and stored Chol was being altered. Cell Chol is found either at cell membranes as FC (mainly at the PM) or stored in lipid droplets as CE. The ratio CE/FC is maintained by the activity of acyl CoA:cholesterol acyltransferase (ACAT), which catalyzes the esterification of FC to different FAs [38,39]. Hence, we sought to establish the effect of FADS over-expression on Chol storage. We measured radioactivity associated to CE and FC after labeling FADS and control cells with [^{3}H] Chol. A small but significantly higher CE/FC ratio was observed in FADS cells (**Fig. 3B**). Previous research has demonstrated that apoA-I induces a decrease of Chol pools available to be esterified by ACAT [40,41]. Thus, Chol removal by overnight incubation with apoA-I turned into a relative decrease of CE in both cell lines.

Effect of FADS over-expression on cell functionality

FC accumulation is cytotoxic, impacting on cell metabolism and viability [39]. To address the effect of desaturases over-expression on cell functionality due to differences in Chol partition, we compared mitochondrial reduction capacity in both cell lines by MTT assay. In a previous work, we have established that MUFA increase by stearoyl-CoA-desaturase over-expression results in greater mitochondrial reduction activity and lower LDH release to the medium suggesting higher cell viability, even after FC load [19]. In the present study, the FADS cells showed 36% greater reduction capacity than the control cells (**Fig. 4**). However, both cell lines were equally sensitive to Chol loading (40% lower OD).

Discussion

PM offers a unique interphase for translating the events from the close environment surrounding the cell to the internal machinery controlling and regulating cell homeostasis in a

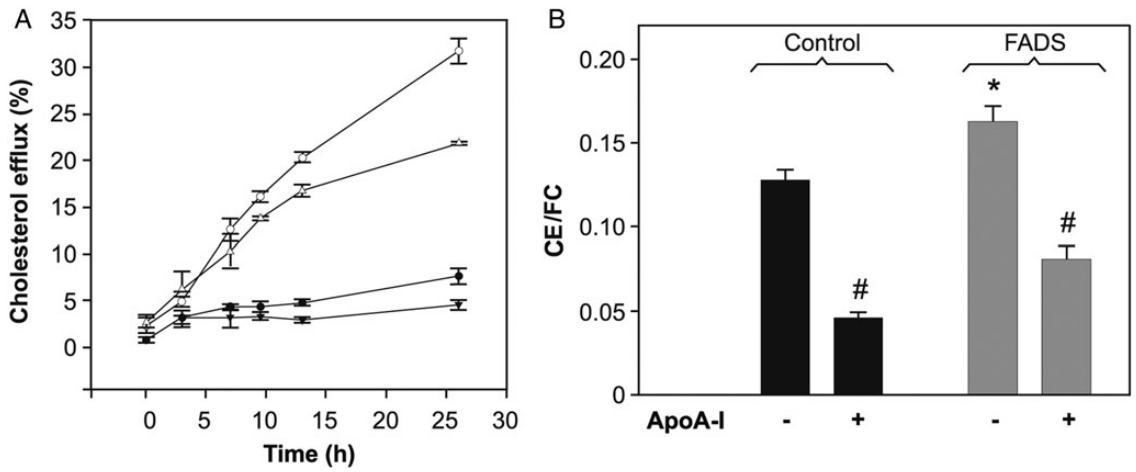

Figure 3. Cholesterol homeostasis (A) Cholesterol efflux was measured by scintilliation counting of [^{3}H] Chol in the incubation medium (methods). Chol efflux from FADS cells towards apoA-I (open triangles) was ~10% less efficient, when compared with the control (open circles) cells. Kinetics showed by close symbols represent efflux measurements from control (circles) and FADS (triangles) cells incubated in the absence of apoA-I. (B) Intracellular Chol esterification. Total lipids were separated by high-performance thin layer chromatography and CE/FC was measured by scintilliation counting of [^{3}H] Chol (methods). Chol removal by overnight incubation with apoA-I (12 μg/ml) resulted in a decrease of CE to a similar extent in both cell lines. $^*P < 0.05$ vs. control cells; $^{\#}P < 0.05$ vs. the same type of cells in the absence of apoA-I.

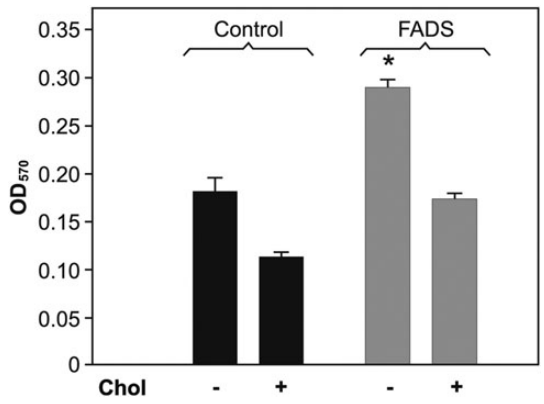

Figure 4. Cellular viability Cell functionality was assayed by MTT (methods). In the absence of Chol, FADS cells (gray bar) showed ~36% greater reduction capacity than the control cells (black bar). Both cell lines were equally sensitive to Chol loading showing 40% lower OD. *$P < 0.05$ vs. control cells.

coordinated fashion. Small changes in physicochemical variables such as Chol content or protein interactions might induce growth or coalescence of certain types of lipid domains, which could in turn modulate membrane-associated physiological signaling. By using synthetic antimicrobial peptides, it was shown that their insertion into the membrane is highly dependent on lipid composition and lateral organization. Phase separation—but not Chol content—has been shown to inhibit peptides activity [42]. It is though that Chol makes fluid domains more rigid thus inhibiting membrane disruption, which is the clue in eukaryotic cells with high Chol content [43]. Interesting studies were achieved by using Pardaxin, a membrane-lysing peptide. While this peptide can promote redistribution of Chol in the PM [44], the addition of Chol in different systems has been found to reduce the peptide's ability to disrupt bilayers, by limiting the backbone motion [45,46].

In other field, it has been suggested that membrane composition is important to determine cytotoxicity associated to amyloid formation. Lipid charge, as well as membrane heterogeneity, curvature, and surface defects can determine peptides insertion into the bilayer and hence the mechanism of membrane disruption [47]. In this trend, it was suggested that the presence of ganglioside enhances both the initial pore formation and fiber-dependent membrane fragmentation, processes that mediate toxicity induced by the Abeta peptide [48].

The delicate balance of the multiple factors participating in PM function is not completely understood and requires to be studied in more details. In a previous work, by using a stable cell line with higher MUFA content in the PM, we proposed the existence of a compensatory mechanism by which cells tend to preserve membrane fluidity in order to maintain functionality [19]. We herein expanded our studies by introducing other permanent perturbations in membrane organization and composition caused by an increase of PUFA. Our results suggested that for cell viability, besides fluidity, the process of redirecting Chol molecules to domains is also important, in which Chol can be solubilized or stored in non-toxic pools.

Membranes with a similar lipid composition were studied by different technical approaches by Wassall *et al*. [11,49]. They simplified PM as lipid rafts floating in a 'sea' of bulk lipids, and showed that PUFA-containing phospholipids have very poor affinity for Chol due to 'high flexibility' attributed to the presence of many unsaturations. They suggested that higher amounts of these lipids segregate Chol apart from the bulk of the membrane, favoring the partition of sterol-rich/SM-rich liquid-ordered regions away from sterol-poor/PUFA-rich liquid domains. GP studies in our present model system (FADS cells) indicated that the more ordered domains keep a similar fluidity (i.e. composition), when compared with the control cells, the more fluid domains (likely enriched in PUFA) become even more fluid. As lower FC content was observed in FADS cells, PM could be then attributed to a decreased amount of Chol solubilized in the more fluid domains. The segregation effect induced by PUFA [11] can favor the existence of a smaller number but of larger size of Chol-rich domains, resulting in a decreased area of surface defects. We have shown that the protein reconstituted in lipid-poor complexes (rHDL) preferentially solubilizes Chol from the more fluid phases [24], but we and others have also suggested previously that apoA-I lipid solubilization from the bilayers is favored by the existence of a large area of surface defects [50,51]. Taken together, these facts could explain why Chol removal mediated by apoA-I is less efficient in these cells, even upon Chol load from an external source (not shown). For more clarity, we represented this hypothesis in a cartoon (**Fig. 5**).

In addition, considering that FC cannot suit properly in a high PUFA level environment, uncomplexed excess Chol should be esterified and stored as CE in order to avoid cell toxicity. Consistent with this, ground state FADS cells showed a higher CE/FC ratio (**Fig. 3**) and greater mitochondrial activity as detected by the MTT assay (**Fig. 4**).

Another mechanism to be considered is that lipid rearrangement at the PM could indeed modify cell-signaling events depending on protein partition into different lipid platforms. PUFA-PL can profoundly alter the 'landscape' of cell membrane lipid rafts/caveolae microdomains, which may directly or indirectly influence Chol removal. Supporting this idea, gene expression of caveolin-1, ABCA1, and SREBP-2 was downregulated by feeding PUFA-enriched diets to dogs with inflammatory bowel disease [52]. A downregulation of caveolin-1 is consistent with the increased ACAT activity suggested by the larger CE content in our cell line [53]. Considering that high FC level is cytotoxic, lower caveolin expression would support the observed increased mitochondrial reduction capacity. We have recently shown

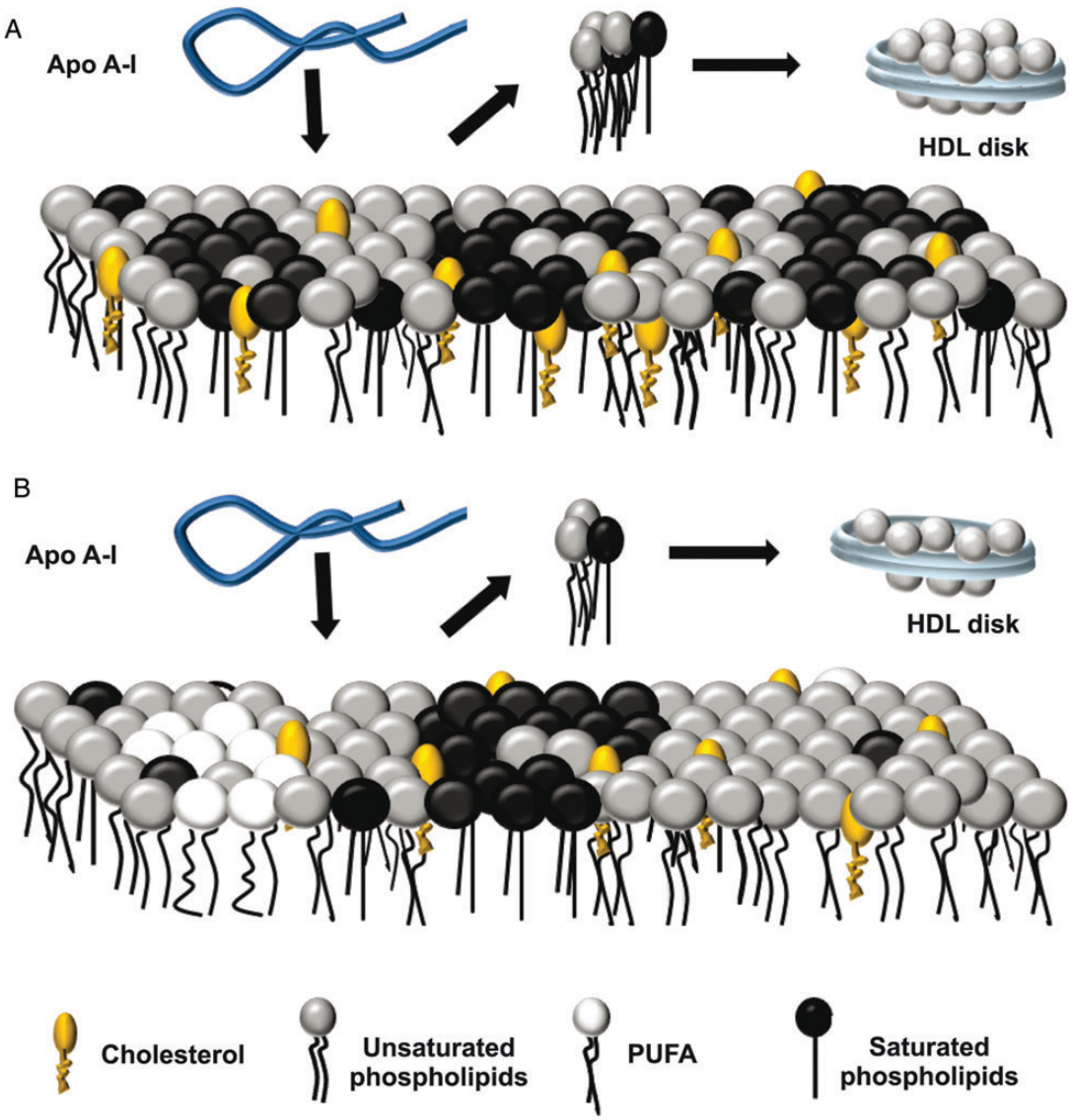

Figure 5. Schematic representation for the interaction of apoA-I with FADS cells membrane (A) Wild-type PM was represented as domains (rafts) enriched in saturated phospholipids (dark circles with straight legs), segregated from areas enriched in unsaturated phospholipids (gray circles with flexible legs) with Chol molecules (orange oval head with one leg) distributed according to their chemical affinities. (B) The increased PUFA (white circles with flexible legs) content in FADS cells enhanced the segregation of Chol into raft domains. This effect together with a lower content of Chol and SM observed in FADS cells would decrease the surface defect area among different domains. Lipid-free apoA-I (blue ribbon) would interact with both types of PM (black arrows in A and B) solubilizing lipids preferentially from the areas with high surface defects giving rise to disk-shaped particles (blue disks). Thus the lower surface areas in the FADS cells would decrease the efficiency of apoA-I to remove lipids.

that Chol extraction from CHO cells membrane decreases the size of GP domains from a range from 300−78 to 78−25 nm, indicating that some ordered domains would split into some smaller ones [51]. Necessarily, our future work will be directed to address the influence of membrane organization on the signaling events involved in cell viability through Chol homeostasis.

Acknowledgements

The authors acknowledge Mr M. Ramos for the assistance with the figures preparation and L. Hernandez for her expertise and technical support with apoA-I purification. M.S.J., M.A.T., M.A.M., and O.J.R. are the members of the Carrera del Investigador Científico (CONICET), Argentina.

Funding

This work was supported by grants from the Agencia Nacional de Promoción Científica y Tecnológica, Argentina (grant number 14443-2003 for O.J.R. and 2106-2008 for M.A.T.), Universidad Nacional de La Plata (grant number M158 for M.A.T.), the Consejo Nacional de Investigaciones Científicas y Técnicas (grant numbers PIP

112-200801-00953 and PIP 112-201101-00648 for M.A.T.), and the National Institutes of Health, USA (grant number PHS 5 P41 RR-03155 for S.A.S.).

References

1. Simopoulos AP. The importance of the omega-6/omega-3 fatty acid ratio in cardiovascular disease and other chronic diseases. Exp Biol Med (Maywood) 2008, 233: 674–688.
2. Sanchez-Muniz FJ, Bastida S, Gutierrez-Garcia O and Carbajal A. Olive oil-diet improves the simvastatin effects with respect to sunflower oil-diet in men with increased cardiovascular risk: a preliminary study. Nutr Hosp 2009, 24: 333–339.
3. Aliche-Djoudi F, Podechard N, Chevanne M, Nourissat P, Catheline D, Legrand P and Dimanche-Boitrel MT, *et al*. Physical and chemical modulation of lipid rafts by a dietary n-3 polyunsaturated fatty acid increases ethanol-induced oxidative stress. Free Radic Biol Med 2011, 51: 2018–2030.
4. Park WJ, Kothapalli KS, Lawrence P and Brenna JT. FADS2 function loss at the cancer hotspot 11q13 locus diverts lipid signaling precursor synthesis to unusual eicosanoid fatty acids. PLoS ONE 2011, 6: e28186.
5. Denis I, Potier B, Vancassel S, Heberden C and Lavialle M. Omega-3 fatty acids and brain resistance to ageing and stress: body of evidence and possible mechanisms. Ageing Res Rev 2013, 12: 579–594.
6. Pallebage-Gamarallage MM, Lam V, Takechi R, Galloway S and Mamo JC. A diet enriched in docosahexanoic Acid exacerbates brain parenchymal extravasation of apo B lipoproteins induced by chronic ingestion of saturated fats. Int J Vasc Med 2012, 2012: 647689.
7. Nakamura MT and Nara TY. Gene regulation of mammalian desaturases. Biochem Soc Trans 2002, 30: 1076–1079.
8. Calder PC. Fatty acids and gene expression related to inflammation. Nestle Nutr Workshop Ser Clin Perform Programme 2002, 7: 19–36.
9. Serhan CN and Savill J. Resolution of inflammation: the beginning programs the end. Nat Immunol 2005, 6: 1191–1197.
10. Huster D, Arnold K and Gawrisch K. Influence of docosahexaenoic acid and cholesterol on lateral lipid organization in phospholipid mixtures. Biochemistry 1998, 37: 17299–17308.
11. Wassall SR and Stillwell W. Polyunsaturated fatty acid-cholesterol interactions: domain formation in membranes. Biochim Biophys Acta 2009, 1788: 24–32.
12. Chapkin RS, Seo J, McMurray DN and Lupton JR. Mechanisms by which docosahexaenoic acid and related fatty acids reduce colon cancer risk and inflammatory disorders of the intestine. Chem Phys Lipids 2008, 153: 14–23.
13. Simons K and Ikonen E. Functional rafts in cell membranes. Nature 1997, 387: 569–572.
14. Laude AJ and Prior IA. Plasma membrane microdomains: organization, function and trafficking. Mol Membr Biol 2004, 21: 193–205.
15. Hancock JF. Lipid rafts: contentious only from simplistic standpoints. Nat Rev Mol Cell Biol 2006, 7: 456–462.
16. Tricerri A, Corsico B, Toledo JD, Garda HA and Brenner RR. Conformation of apolipoprotein AI in reconstituted lipoprotein particles and particle-membrane interaction: effect of cholesterol. Biochim Biophys Acta 1998, 1391: 67–78.
17. Zolfaghar R, Cifelli CJ, Banta MD and Ross AC. Fatty acid delta(5)-desaturase mRNA is regulated by dietary vitamin A and exogenous retinoic acid in liver of adult rats. Arch Biochem Biophys 2001, 391: 8–15.
18. Aki T, Shimada Y, Inagaki K, Higashimoto H, Kawamoto S, Shigeta S and Ono K, *et al*. Molecular cloning and functional characterization of rat delta-6 fatty acid desaturase. Biochem Biophys Res Commun 1999, 255: 575–579.
19. Jaureguiberry MS, Tricerri MA, Sanchez SA, Garda HA, Finarelli GS, Gonzalez MC and Rimoldi OJ. Membrane organization and regulation of cellular cholesterol homeostasis. J Membr Biol 2010, 234: 183–194.
20. Mander EL, Dean RT, Stanley KK and Jessup W. Apolipoprotein B of oxidized LDL accumulates in the lysosomes of macrophages. Biochim Biophys Acta 1994, 1212: 80–92.
21. Mosmann T. Rapid colorimetric assay for cellular growth and survival: application to proliferation and cytotoxicity assays. J Immunol Methods 1983, 65: 55–63.
22. Bagatolli LA, Sanchez SA, Hazlett T and Gratton E. Giant vesicles, Laurdan, and two-photon fluorescence microscopy: evidence of lipid lateral separation in bilayers. Methods Enzymol 2003, 360: 481–500.
23. Parasassi T and Gratton E. Membrane lipid domains and dynamics as detected by Laurdan fluorescence. J Fluoresc 1995, 8: 365–373.
24. Sanchez SA, Tricerri MA and Gratton E. Interaction of high density lipoprotein particles with membranes containing cholesterol. J Lipid Res 2007, 48: 1689–1700.
25. Sanchez SA, Tricerri MA, Gunther G and Gratton E. Laurdan generalized polarization: from cuvette to microscope. Modern research and educational topics in microscopy. Appl Phys Chem Sci 2007, 1: 1007–1014.
26. Weber G and Farris FJ. Synthesis and spectral properties of a hydrophobic fluorescent probe: 6-propionyl-2-(dimethylamino)naphthalene. Biochemistry 1979, 18: 3075–3078.
27. Parasassi T, Gratton E, Yu WM, Wilson P and Levi M. Two-photon fluorescence microscopy of Laurdan generalized polarization domains in model and natural membranes. Biophys J 1997, 72: 2413–2429.
28. So PTC, French T, Yu WM, Berland KM, Dong CY and Gratton E. Time resolved fluorescence microscopy using two photon excitation. Bioimaging 1995, 3: 49–63.
29. Sanchez SA, Bagatolli LA, Gratton E and Hazlett TL. A two-photon view of an enzyme at work: crotalus atrox venom PLA2 interaction with single-lipid and mixed-lipid giant unilamellar vesicles. Biophys J 2002, 82: 2232–2243.
30. Tricerri MA, Toledo JD, Sanchez SA, Hazlett TL, Gratton E, Jonas A and Garda HA. Visualization and analysis of apolipoprotein A-I interaction with binary phospholipid bilayers. J Lipid Res 2005, 46: 669–678.
31. Sanchez SA, Tricerri MA, Ossato G and Gratton E. Lipid packing determines protein-membrane interactions: challenges for apolipoprotein A-I and high density lipoproteins. Biochim Biophys Acta 2010, 1798: 1399–1408.
32. Harris FM, Best KB and Bell JD. Use of laurdan fluorescence intensity and polarization to distinguish between changes in membrane fluidity and phospholipid order. Biochim Biophys Acta 2002, 1565: 123–128.
33. Navarro-Lerida I, Sanchez-Perales S, Calvo M, Rentero C, Zheng Y, Enrich C and Del Pozo MA. A palmitoylation switch mechanism regulates Rac1 function and membrane organization. Embo J 2012, 31: 534–551.
34. Sanchez SA, Gunther G, Tricerri MA and Gratton E. Methyl-beta-cyclodextrins preferentially remove cholesterol from the liquid disordered phase in giant unilamellar vesicles. J Membr Biol 2011, 241: 1–10.
35. Heiner AL, Gibbons E, Fairbourn JL, Gonzalez LJ, McLemore CO, Brueseke TJ and Judd AM, *et al*. Effects of cholesterol on physical properties of human erythrocyte membranes: impact on susceptibility to hydrolysis by secretory phospholipase A2. Biophys J 2008, 94: 3084–3093.
36. Mendez AJ, Lin G, Wade DP, Lawn RM and Oram JF. Membrane lipid domains distinct from cholesterol/sphingomyelin-rich rafts are involved in the ABCA1-mediated lipid secretory pathway. J Biol Chem 2001, 276: 3158–3166.
37. Hayashi M, Abe-Dohmae S, Okazaki M, Ueda K and Yokoyama S. Heterogeneity of high density lipoprotein generated by ABCA1 and ABCA7. J Lipid Res 2005, 46: 1703–1711.
38. Lange Y and Steck TL. Cholesterol homeostasis and the escape tendency (activity) of plasma membrane cholesterol. Prog Lipid Res 2008, 47: 319–332.

39. Warner GJ, Stoudt G, Bamberger M, Johnson WJ and Rothblat GH. Cell toxicity induced by inhibition of acyl coenzyme A: cholesterol acyltransferase and accumulation of unesterified cholesterol. J Biol Chem 1995, 270: 5772–5778.
40. Yamauchi Y, Chang CC, Hayashi M, Abe-Dohmae S, Reid PC, Chang TY and Yokoyama S. Intracellular cholesterol mobilization involved in the ABCA1/apolipoprotein-mediated assembly of high density lipoprotein in fibroblasts. J Lipid Res 2004, 45: 1943–1951.
41. Gonzalez MC, Toledo JD, Tricerri MA and Garda HA. The central type Y amphipathic alpha-helices of apolipoprotein AI are involved in the mobilization of intracellular cholesterol depots. Arch Biochem Biophys 2008, 473: 34–41.
42. McHenry AJ, Sciacca MF, Brender JR and Ramamoorthy A. Does cholesterol suppress the antimicrobial peptide induced disruption of lipid raft containing membranes? Biochim Biophys Acta 2012, 1818: 3019–3024.
43. Brender JR, McHenry AJ and Ramamoorthy A. Does cholesterol play a role in the bacterial selectivity of antimicrobial peptides? Front Immunol 2012, 3: 195.
44. Epand RF, Ramamoorthy A and Epand RM. Membrane lipid composition and the interaction of pardaxin: the role of cholesterol. Protein Pept Lett 2006, 13: 1–5.
45. Hallock KJ, Lee DK, Omnaas J, Mosberg HI and Ramamoorthy A. Membrane composition determines pardaxin's mechanism of lipid bilayer disruption. Biophys J 2002, 83: 1004–1013.
46. Ramamoorthy A, Lee DK, Narasimhaswamy T and Nanga RP. Cholesterol reduces pardaxin's dynamics—a barrel-stave mechanism of membrane disruption investigated by solid-state NMR. Biochim Biophys Acta 2010, 1798: 223–227.
47. Brender JR, Salamekh S and Ramamoorthy A. Membrane disruption and early events in the aggregation of the diabetes related peptide IAPP from a molecular perspective. Acc Chem Res 2012, 45: 454–462.
48. Sciacca MF, Kotler SA, Brender JR, Chen J, Lee DK and Ramamoorthy A. Two-step mechanism of membrane disruption by Abeta through membrane fragmentation and pore formation. Biophys J 2012, 103: 702–710.
49. Wassall SR, Brzustowicz MR, Shaikh SR, Cherezov V, Caffrey M and Stillwell W. Order from disorder, corralling cholesterol with chaotic lipids. The role of polyunsaturated lipids in membrane raft formation. Chem Phys Lipids 2004, 132: 79–88.
50. Pownall HJ, Massey JB, Kusserow SK and Gotto AM, Jr. Kinetics of lipid—protein interactions: interaction of apolipoprotein A-I from human plasma high density lipoproteins with phosphatidylcholines. Biochemistry 1978, 17: 1183–1188.
51. Sanchez SA, Tricerri MA and Gratton E. Laurdan generalized polarization fluctuations measures membrane packing micro-heterogeneity *in vivo*. Proc Natl Acad Sci USA 2012, 109: 7314–7319.
52. Ontsouka CE, Burgener IA, Mani O and Albrecht C. Polyunsaturated fatty acid-enriched diets used for the treatment of canine chronic enteropathies decrease the abundance of selected genes of cholesterol homeostasis. Domest Anim Endocrinol 2009, 38: 32–37.
53. Frank PG, Cheung MW, Pavlides S, Llaverias G, Park DS and Lisanti MP. Caveolin-1 and regulation of cellular cholesterol homeostasis. Am J Physiol Heart Circ Physiol 2006, 291: 677–686.